Research, Society and Development, v. 10, n. 5, e45310515017, 2021
(CC BY 4.0) | ISSN 2525-3409 | DOI: http://dx.doi.org/10.33448/rsd-v10i5.15017

In vivo transdifferentiation, osteoconductive and osteoinductive properties of experimental water-soluble organo-biomaterials – A Pilot Study

Propriedades de transdiferenciação, osteocondução e osseoindução in vivo de biomateriais orgânicos experimentais solúveis em água – Estudo Piloto

Propiedades de transdiferenciación, osteoconducción y osteoinducción in vivo de biomateriales orgánicos experimentales soluble en agua – Estudio Piloto

Received: 04/13/2021 | Reviewed: 04/21/2021 | Accept: 04/28/2021 | Published: 05/17/2021

Viviane Rozeira Crivellaro
ORCID: https://orcid.org/0000-0002-0601-3350
Positivo University, Brazil
E-mail: anecrivellaro@hotmail.com
Gilvan Spada
ORCID: https://orcid.org/0000-0002-1835-0098
Positivo University, Brazil
E-mail: gilvanspada@hotmail.com
Cláudia Salete Judachesci
ORCID: https://orcid.org/0000-0002-5580-7958
Positivo University, Brazil
E-mail: claudia_judachesci@hotmail.com
Paula Porto Spada
ORCID: https://orcid.org/0000-0002-3143-5467
Positivo University, Brazil
E-mail: portopaula@hotmail.com
Luiza Rodrigues Saling
ORCID: https://orcid.org/0000-0002-8484-4934
Positivo University, Brazil
E-mail: luiza_saling@hotmail.com
Idélcena Tatiane Miranda
ORCID: https://orcid.org/0000-0002-7397-3837
Positivo University, Brazil
E-mail: idelcena@gmail.com
Tatiana Miranda Deliberador
ORCID: https://orcid.org/0000-0003-4076-4905
Positivo University, Brazil
E-mail: tdeliberador@gmail.com
Marilisa Carneiro Leão Gabardo
ORCID: https://orcid.org/0000-0001-6832-8158
Positivo University, Brazil
E-mail: marilisagabardo@gmail.com
Rafaela Scariot
ORCID: https://orcid.org/0000-0002-4911-6413
Federal University of Paraná, Brazil
E-mail: rafaela_scariot@yahoo.com.br
Moira Pedroso Leão
ORCID: https://orcid.org/0000-0003-3724-911X
Curityba Biotech LTDA, Brazil
E-mail: moirapedroso@gmail.com
Carmen Lucia Mueller Storrer
ORCID: https://orcid.org/0000-0002-1188-8848
Positivo University, Brazil
E-mail: carmen.storrer@gmail.com
Sharukh Soli Khajotia
https://orcid.org/0000-0001-8171-0474
University of Oklahoma, United States
E-mail: sharukh-khajotia@ouhsc.edu

Fernando Luis Esteban Florez
ORCID: https://orcid.org/0000-0002-8351-0721
University of Oklahoma, United States
E-mail: fernando-esteban-florez@ouhsc.edu
João César Zielak
ORCID: https://orcid.org/0000-0003-3393-3491
Positivo University, Brazil
E-mail: jzielak2@gmail.com

Abstract
Inorganic bovine bone matrix (IBBM) is a biomaterial with proven osteoconductive functionalities. The objective of this study was to assess the in vivo bone regeneration functionalities of IBBM modified or not by an experimental MOE in sheep. MOE synthesis was performed by suspending nacre particles (0.05 g, diameters < 0.01 mm) in anhydrous acetic acid (pH 7, 5 mL, 25°C, 72 hours) using magnetic stirring. Polyethylene carriers (d= 5.0 mm, l= 10.0 mm, open ends) of negative control (sham) or experimental groups (IBBM or MOE-modified IBBM) were placed (n=3 conditions /animal; intramuscularly) adjacent to the lower spine of adult sheep (8 animals, ≈ 45 Kg, 2 years old). Tissues were harvested (at 3 or 6 months) after implantation in preparation for histological (H), morphometrical (MM) and immunohistochemical analyses (IH; Wnt-3a, CD34, Vimentin and PREF-1). MM data were tested for normality and variance homogeneity using the Shapiro-Wilk and Levene tests, and Mann Whitney and Kruskal-Wallis, respectively. IM data were analyzed using two-way ANOVA and Tukey tests. Differences ($p < 0.05$) were observed between experimental groups (IBBM and IBBM+MOE at both 3 and 6 months) and controls (sham) for total area; Differences were not found for presence of remnant particles among experimental groups. The highest formation of bone was observed with IBBM+MOE (6-months). No differences ($p > 0.05$) were found on IM analysis (CD34, Vimentin, PREF-1, Wnt3a). Results indicated that experimental materials (IBBM+MOE) display promising functionalities. Additional studies are necessary to define biomaterials' longitudinal effects and long-term biocompatibility properties.
Keywords: Tissue engineering; Organic; Biomaterials; Ectopic grafting; Bone regeneration; Immunohistochemical.

Resumo
A matriz óssea inorgânica bovina (IBBM) é um biomaterial com funcionalidades osteocondutoras comprovadas. Este estudo avaliou as funcionalidades ósseo-regenerativas do IBBM modificado ou não por MOE em ovinos. MOE foi sintetizado através da suspensão do nacre (0.05 g, diâmetros < 0.01 mm) em ácido acético anidro (pH 7, 25°C, 72 horas) usando agitação magnética. Tubos de polietileno (d = 5.00 mm, c = 10.0 mm, extremidades abertas) do controle negativo (sham) ou grupos experimentais (IBBM ou IBBM modificado por MOE) foram posicionados (n = 3/condição/animal; intramuscular) adjacentes á distal da coluna de ovelhas (8 animais, ≈ 45 Kg, 2 anos). Tecidos foram colhidos (3 ou 6 meses) pós-implantação para análises histológicas (H), morfométricas (MM) e imunohistoquímicas (IH; Wnt-3a, CD34, Vimentin and PREF-1). Dados MM foram analisados utilizando os testes Shapiro-Wilk e Levene, Mann Whitney e Kruskal-Wallis. Dados IM foram analisados usando ANOVA de medidas repetidas e Tukey. Diferenças ($p < 0.05$) foram observadas entre of grupos experimentais (IBBM e IBBM + MOE aos 3 e 6 meses) e controles (sham) para área total; não foram encontradas diferenças para partículas remanescentes entre os grupos experimentais; osso neoformado ocorreu apenas na presença de biomateriais. Os maiores valores de osso neoformado foram observados com IBBM + MOE (6-meses). Diferenças estatísticas ($p > 0.05$) não encontradas na análise IM (Wnt-3a, CD34, Vimentin and PREF-1). Resultados indicam que materiais experimentais (IBBM + MOE) apresentam funcionalidades promissoras. Estudos adicionais são necessários para definir os efeitos longitudinais dos biomateriais e suas propriedades de biocompatibilidade de longo prazo.
Palavras chave: Engenharia de tecidos; Orgânico; Biomateriais; Enxerto ectópico; Regeneração óssea; Imunohistoquímica.

Resumen
Matriz ósea inorgánica bovina (IBBM) son biomateriales con características osteocoductoras comprobadas. El objetivo del presente fue evaluar las funcionalidades de regeneración ósea de IBBM modificado por MOE en ovinos. MOE fue sintetizado suspendiendo-se nácar (0.05 g, diámetros < 0.01 mm) en ácido acético anhidro (pH 7, 25° C, 72 horas) con agitación magnética. Tubos huecos de polietileno (d = 5.00 mm, l = 10.00 mm, extremos abiertos) del grupo control negativo (simulacro) o grupos experimentales (IBBM o IBBM modificado por MOE) fueran colocados (n = 3/condición/animal; intramuscular) adyacente a la parte distal de la columna de ovejas (8 animales, ≈ 45 kg, 2 años). Tejidos fueron recogidos (3 o 6 meses) después implantación para análisis histológicos (H), morfométricos (MM) e inmunohistoquímicos (IH; Wnt-3a, CD34, Vimentin y PREF-1). Datos MM se analizaron utilizando las pruebas de Shapiro-Wilk y Levene, Mann Whitney y Kruskal Wallis. Datos IM se analizaron mediante ANOVA de medidas repetidas y Tukey. Diferencias ($p < 0.05$) ocurrieran entre grupos experimentales (IBBM y IBBM +MOE a los 3 y 6 meses) y controles (simulacro) para área total; no se encontraron diferencias para partículas remanentes entre grupos experimentales; hueso recién formado se produjo solo en

la presencia de biomateriales. Maior cantidad de hueso fue observada con IBBM + MOE (6-meses). No hubo diferencias (p > 0.05) en IH (Wnt-3a, CD34, Vimentin y PREF-1). Resultados reportados indican que materiales experimentales (IBBM + MOE) tienen características prometedoras. Se necesitan estudios para definir efectos longitudinales y de biocompatibilidad de los biomateriales.
Palabras clave: Ingeniería de tejidos; Orgánica; Biomateriales; Injerto ectópico; Regeneración ósea; Inmunohistoquímica.

1. Introduction

Inorganic bovine bone matrix (IBBM) is an implantable biomaterial with osteoconductive properties that are promising for the development of novel in vivo bone regeneration strategies. These 3-dimensional scaffolds should facilitate the ingress and growth of undifferentiated and pluripotent stem cells (hPSCs), and should have adequate properties (mechanical, chemical and biological) to passively guide the growth of bony tissues, whereby organic and inorganic components of the matrix, are resorbed to allow the concurrent deposition of bone. (Carvalho et al., 2004) According to Wilson-Hench, (Donaruma, 1988) osteoconduction is the process by which newly-formed bony tissues are directed to conform over a material's surface. Martín-Moldes et al. (Martín-Moldes et al., 2018) while investigating the cellular mechanisms involved in bone regeneration precipitated by recombinant DNA sequences, indicated that IBBM can be used in association with osteoinductive biomaterials to stimulate the differentiation of mesenchymal cells into osteoblasts and osteocytes.

The underlying molecular mechanisms involved in bone neoformation started to be investigated (in animal models) in the mid 1960s, when Urist (Urist, 1965) observed the reaction of intramuscular tissues after the placement of demineralized (partially of wholly) bone matrix implants. A previous report (Urist & Strates, 1970) indicate that such implantation model display favorable histological characteristics (e.g., abundant vascularization), limit the mechanical interference of the host, can be used in biocompatibility assessments, and ectopic sites, are typically used to determine the osteoinductive properties of implantable biomaterials. Other studies investigating the regeneration functionalities of bone graft materials (biphasic calcium phosphates or Teflon capsules), associated or not with recombinant human platelet-derived growth factor, have validated the utilization of muscular tissues for the assessment of biocompatibility and osteoinductive functionalities of novel implantable biomaterials (Habibovic et al., 2008; Lioubavina-Hack et al., 2005).

The formation of bone within muscular tissues is believed to be induced by epigenetic modifications in canonical pathways that control the trans-differentiation of non-osteogenic cells (i.e., fibroblasts or pre-adipocytes) into osteoblasts. (Cho et al., 2014) Wingless-type glycoproteins (Wnt; e.g., Wnt-3a and Wnt-10b) comprise a family of excreted signaling proteins capable of regulating several developmental processes (in vitro and in vivo), (Bennett et al., 2005; Minear et al., 2010) where high Wnt levels are associated with the neoformation of bone, and low Wnt concentrations may indicate the loss of bone (Miclea et al., 2010; Morvan et al., 2006) due to a decrease in osteogenic potential (Jing et al., 2015).

A previous study demonstrated the presence and the activity of hPSCs in skeletal muscle cells (SMCs), where pluripotent differentiation capabilities were observed even after long periods of time (Reimann et al., 2004). According to Lee et al. (2011) and Beauchamp et al. (2000) these types of cells can be characterized by their positive response to the antibody CD34 at the membrane of satellite cells (Nogami, 2018). Akiyama et al. (2018) while investigating the differentiation of human pluripotent cells into skeletal muscle, stated that human induced stem cells (hiPSCs), have the potential to essentially differentiate into all types of human cells. Other studies (Jasani, 2000; Lagace et al., 1985) have demonstrated that fibroblasts and pre-adipocytes also display potential for trans-differentiation, and suggested that Vimentin (58 kD, intermediary filament-type protein) (Fhied et al., 2014) and pre-adipocyte factor (Pref- 1, transmembrane-type protein) (Wang & Cooke, 2005) can be used during the identification of mesenchymal cells.

A recent study investigating the in vivo regeneration functionalities of experimental organo-biomaterials containing water-soluble nacre extracts (Zielak et al., 2018) reported a simple method for the fabrication of experimental implantable biomaterials with favorable osteoinductive and osteogenic properties. According to Addadi et al. (2006) and Huang and Li (2012) nacre has attracted wide spread interest in biomineralization studies because of its unique self-assembled hierarchical structure based on a naturally-occurring nanocomposite composed by polygonal aragonite platelets (thickness between 200-500 nm) and interlamellar layers of a water-soluble organic biopolymer. Such nanostructured material display specific mechanical (fracture toughness) and biological properties (bioactivity and mineralization) that are similar to those observed in human bones (Asvanund, 2011; de Almeida, 2011; Duplat et al., 2007; Rousseau, 2011). Other studies investigating the osteoinductive effects of subcutaneous nacre implants in rats, have shown that implants investigated were capable to recruit and promote differentiation of fibroblasts into chondrocyte cells due to the presence of diffusible bone morphogenic proteins (BMPs) (Atlan et al., 1997; Lopez, 1996; Lopez et al., 1992; Silve et al., 1992). Therefore, based on the context presented, the objective of the present study was to comprehensively investigate using histological, histomorphometric and immunohistochemical analyses, the osteoinductive properties of IBBMs modified by experimental MOEs.

2. Methodology

2.1 Internal Review Board (IRB)

The present in vivo pilot study was reviewed and approved by the Internal Review Board of the Positivo University (protocol # CEUA 21/11). The guidelines for the handling and usage of laboratory animals recommended by the European Community were followed in the present study. The present pilot study was conducted based on methodologies previously described by Le Nihouannen et al. (2005), da Silva et al. (2016) and Zielak et al. (2018).

2.2 Manufacturing of Marine organic extract (MOE)

The water-soluble experimental MOE investigated in the present study was obtained from the internal nacre lining of bivalve mollusks (*Perna perna*). The manufacturing process has been described in details in a previous publication from our laboratory (Zielak et al., 2018). In brief, intact shells of whole and frozen brown mussels were reduced into fine particles (size distribution < 0.01 mm) with a planetary ball mill (AMEF, São Paulo, Brazil). Individual portions (0.05 g) of the loose powder were then suspended in anhydrous acetic acid (pH 7, 5.0 mL, room temperature) for 72 hours using external magnetic stirring. The experimental MOE was then separated from suspended particles by centrifugation and stored under refrigeration (4°C) until further use.

2.3 Design of Experiments

According to Le Nihouannen et al. (2005), same herd sheep (total of 8 animals) were selected to participate in the present randomized in vivo pilot study. Each sheep had 2 years of age and weighed around 45 kg. A computer software (Research Randomizer [version 4.0], Social Psychology Network, U.S.A.; available at www.randomizer.org/form.htm) was used to randomly distribute the selected sheep into 6 different experimental groups, such as: G1 (Sham 3 months, S3), G2 (IBBM 3 months, IBBM3), G3 (IBBM + MOE 3 months, IBBM+MOE3), G4 (Sham 6 months, S6), G5 (IBBM 6 months, IBBM6), and G6 (IBBM + MOE 6 months, IBBM+MOE6). Each animal received a total of 3 sterile non-reactive polyethylene tubes (diam. = 5.0 mm x length = 10.0 mm, with both ends open) following previously published protocols (da Silva et al., 2016; Zielak et al., 2018). Experimental groups

G1 and G4 served as the negative control (empty tubes), while groups G2 and G5 served as the positive control (tubes containing unaltered IBBM [GenOx Inorg®, Baumer, Brazil]). Polyethylene tubes of G3 and G6 contained IBBM modified by 40 μL of MOE (Zielak et al., 2018). Throughout the course of the present study, animals were identified using earrings, as it is commonly done in traditional farming procedures. Sheep were grass-fed and had access to water without any restrictions. Table 1 describes the experimental conditions of the present study.

Table 1. Experimental conditions; Sham = empty tube; MOE = Marine organic extract; IBBM = Inorganic bovine bone matrix.

Groups	Type	Monitoring Time	Biomaterial (abbreviation)
1	Control	3 months (4 animals)	Sham (S3)
2	Experimental		IBBM (IBBM3)
3	Experimental		IBBM + MOE (IBBM+MOE3)
4	Control	6 months (4 animals)	Sham (S6)
5	Experimental		IBBM (IBBM6)
6	Experimental		IBBM + MOE (IBBM+MOE6)

Source: Authors (2021).

Table 1 shows the groups divided by treatment, but for each monitoring time (3 and 6 months) there were 4 animals who received 3 tubes at the same time: the first tube was called Sham, which was the control, an empty tube, with no biomaterial; the second tube had the pure biomaterial (IBBM); and the third tube received the biomaterial associated with the marine extract (IBBM + MOE).

2.4 Surgical implantation procedures

Water and solid food were restricted respectively at 6-8 and 24 hours prior to the execution of surgical procedures. At the surgery day, the described protocol was followed: animals received an intramuscular injection of pre-anesthetic medication (Acepromazine, 0.55 mg/Kg, Vetnil, Brazil; Ketamine 20 mg/Kg, Vetbrands, Brazil). After that, anesthesia was intravenously administered to animals (sodium thiopental, 5 mg/Kg, Zeneca Farmacêutica, Brazil), and animals' sedation was sustained using isoflurane via oxygen vaporization (3 L/min., Biochimico, Brazil). During the surgery, Ketoprofen (10%, Biofarm Química e Farmacêutica Ltda., Brazil) and enrofloxacin (10%, Chemitec Agro Veterinária, Brazil) were administered to animals (concentrations of 3.0 mg/Kg and 2.5 mg/K, respectively) using a catheter placed at the marginal ear vein. After trichotomy, surgical sites were decontaminated using povidone-iodine (10%, PVPI, Rioquímica, Brazil), and were delineated 3.0 cm cranially to the sacral promontory, 6.0 cm laterally (to vertebral column) and extended cranially (20.0 cm). Three perpendicular incisions (to vertebral column; ≈ 3.0 cm/ each, 4 cm apart) on the dermis were randomly performed (right or left side) to expose the muscular fascia (*Longissimus dorsi*). Additional intramuscular incisions (1.0 cm/each) were made parallel to the vertebral column to allow for the separation of muscular fibers and the placement of the sterile polyethylene tubes pertaining to each group investigated as described in Table 1. Suture of the muscular fascia and external dermis was performed using resorbable (Vicryl 5-0, Ethicon, Brazil) and non-

resorbable (Nylon 5-0, Shalon Fios Cirúrgicos Ltda. Brazil) materials following a previously published protocol (Zielak et al., 2018). After surgery, animals received intramuscular injections of 10% Ketoprofen (3.0 mg/Kg, Biofarm Química e Farmacêutica Ltda., Brazil) and 10% Enrofloxacin (2.5 mg/Kg, Chemitec Agro Veterinária, Brazil) for 3 and 5 days, respectively.

2.5 Euthanasia of animals

Three or six months after surgery, participating animals were subjected to euthanasia procedures following a protocol previously described by our research group (Zielak et al., 2018). Briefly, sodium thiopental (8 mg/Kg, Thiopentax, Cristália, Brazil) and potassium chloride (19:1 *in bolus*; 20.0 mL, Ariston, Brasil) were administered intravenously and parenterally, respectively, to allow for the harvesting of excisional biopsy of tissues (≈ 1.0 cm adjacent to implants) containing experimental materials and non-reactive carriers (tubes).

2.6 Preparation of tissues for histologic, morphometric and immunohistochemical analyses

Biopsied tissues were immediately placed in individual vials containing formalin (10%, neutral, buffered, 50 mL /vial, 4°C; Sigma-Aldrich, Brazil) to allow the fixation of neoformed tissues inside the non-reactive carriers. After 48 hours, individual specimens were decalcified in trichloroacetic acid (TCA) for 40 days. Tissues were then incorporated into blocks of paraffin and were serially sectioned (6 μm/slice). A portion of prepared slides was treated with Masson's trichrome stain (MTS) in preparation for histologic and morphometric analyses, while the remaining portion of slides was prepared for traditional immunohistochemical assessment.

2.7 Histologic and morphometric analyses

Samples were recovered intact from the tubes. After that, samples were subjected to serial slicing following the long axis of the sample. The most central slice from each sample investigated was then chosen and mounted onto slides for histologic and morphometric analyses. Each slide was imaged 3 times (each time using 3 magnifications [40 ×, 100 × and 400 ×, respectively) using a (BX 41, Olympus Optical Company, Japan) and a digital camera (Canon T31, Japan). Acquired images were then assessed for "total area", "remnant particles" and "bone neoformation" using Photoshop CS4 (adobe Systems Inc., U.S.A.) and ImageJ (National Institutes of Health, U.S.A; freeware available at http://imagej.nih.gov/ij/).

2.8 Immunohistochemical analysis

Slides were prepared according to manufacturer's instructions using the antibodies Wnt-3a, CD34 and vimentin from Santa Cruz Biotechnology (U.S.A.) and Human Pref-1 (DLK, Abcam, U.S.A.) and imaged (400 × magnification, 3 images/slide; 1 at central area, 2 at peripheral regions) with an optical microscope (BX 41, Olympus Optical Company, Japan) coupled with a digital camera (Canon T31, Japan). Acquired images were then assessed using Photoshop CS4 and ImageJ, as previously described.

2.9 Statistical Analysis

All data obtained were tested for normality and variance homogeneity using the Kolmogorov-Smirnov and Levene tests, respectively. Since immunohistochemical data set was normally distributed, the obtained data was then analyzed using the two-factor ANOVA and Tukey parametric tests to determine the presence of significant statistical differences ($p < 0.05$) across experimental groups investigated. A statistical analysis software (SPSS®, version 21.0, International Business Machine, U.S.A.) was used to perform all statistical analyses in the present study.

3. Results

3.1 Histological findings

Figure 1 (A-F) illustrates the histological results from the negative control groups (S3 and S6), where it is possible to observe that empty implants of non-reactive polyethylene tubes (Sham) at 3 or 6 months, were not able of promoting mineralized tissues neoformation. Instead, findings indicate that these implants investigated promoted the formation of fibrous connective tissues displaying organized matrixes and collagen bundles oriented parallel to the longitudinal axis of the implants. In addition to that, it is also possible to observe on Figure 1 (D-F) that implants of S6 displayed higher quantities of tissues from connective and vascular origins, thereby indicating that tissues became denser and more organized 6 months after surgery.

Figure 1. Masson trichrome colored histology images from groups 1 and 4 (control). Images A-C correspond to Sham at 3 months. Images E-F correspond to Sham at 6 months. In both cases, images are presented in terms of increasing magnification (40 ×, 100 × and 400 ×, respectively). Star = Dense connective tissue; Pyramid = Neovascularization; Diamonds = Non-collagenous fibrils.

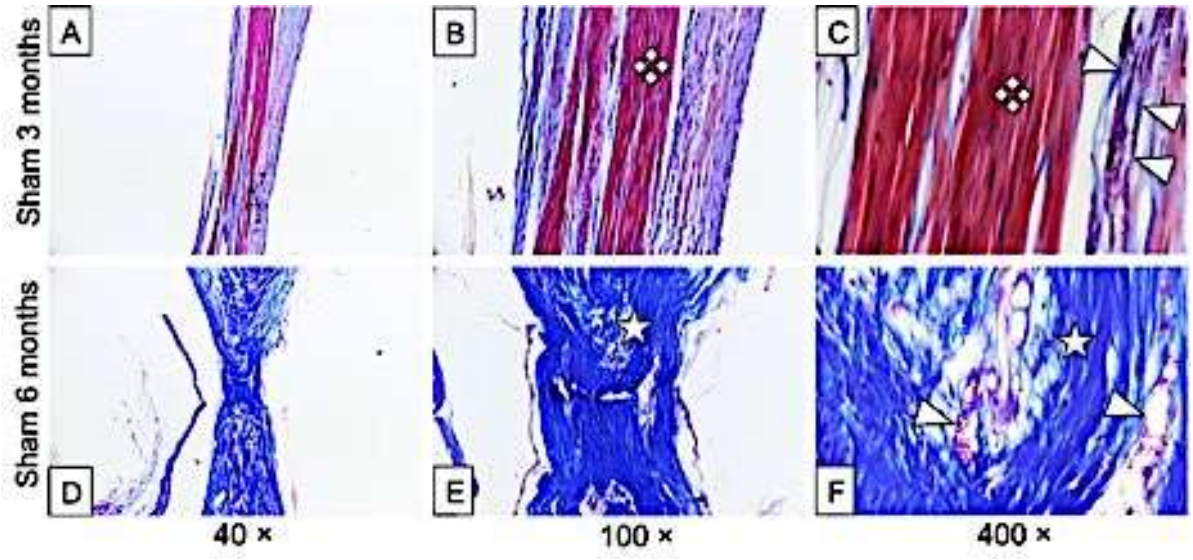

Source: Authors (2021).

Again, Figure 1A shows a connective tissue in 40 × magnification, which can be better viewed in the next two, Figure 1B (100 × magnification) and Figure 1C (400 × magnification). All demonstrating the initial biological local response to the insertion of the empty tube (Sham = control). Figures 1D (40 × magnification), 1E (100 × magnification) and 1F (400 × magnification) demonstrate the local response after 6 months of the empty tube insertion in the animal muscle, showing a dense connective tissue surrounded by blood vessels.

Figure 2 (A-D) illustrates the results from experimental groups IBBM3 and IBBM6. Figure 2 (A and B) allows the observation of large quantities of remnant IBBM particles surrounded by an osteoid matrix and sparse immature bone (IB) after 3 months of implantation. Figure 2 (C and D) shows that unaltered IBBM were capable to promote the formation of small quantities of neoformed mature bone 6 months after implantation, however the presence of osteoid matrix or IB could not be observed.

Figure 2. Masson trichrome colored histology images from groups 2 and 5 (IBBM). Images A-B correspond to IBBM at 3 months. Images C-D correspond to IBBM at 6 months. In both cases, images are presented in terms of increasing magnification (40 × and 200 ×, respectively). IBM = Inorganic bone matrix (or IBBM); Star = Dense connective tissue; NB = Mature neoformed bone; P = Graft particles; IB = Immature bone.

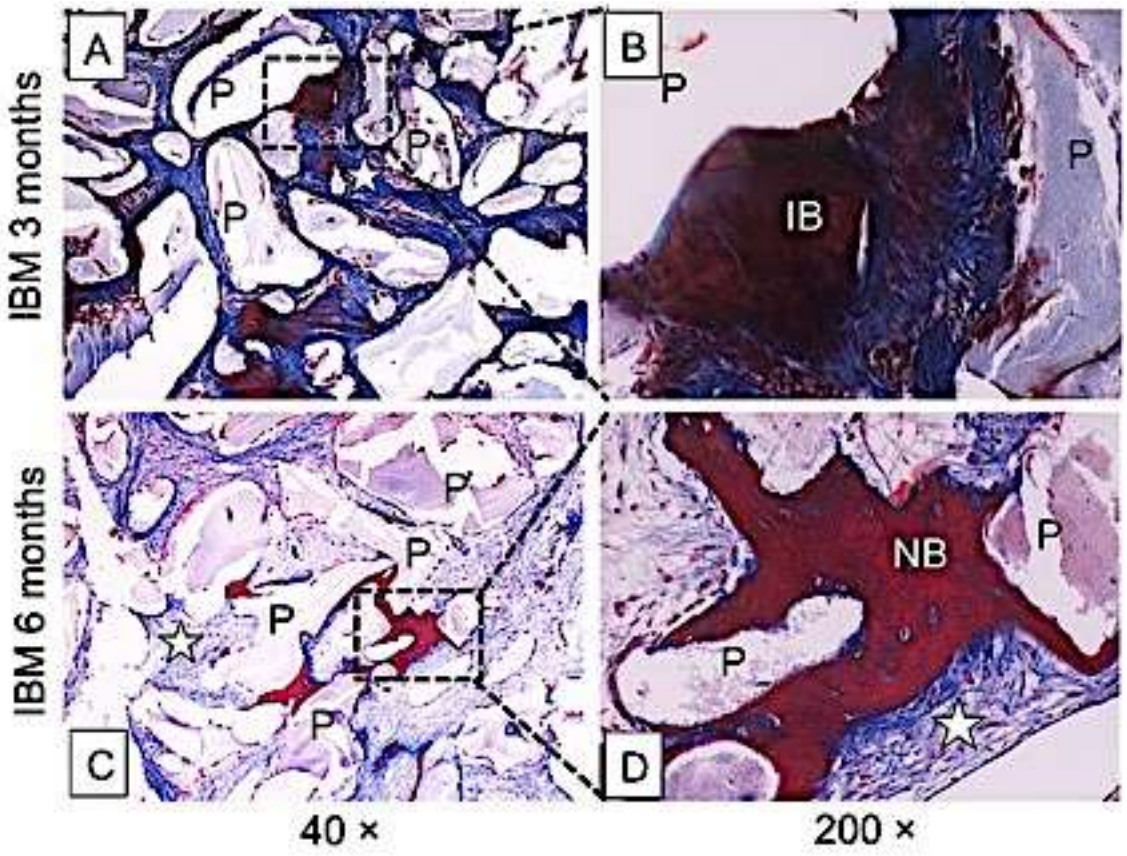

Source: Authors (2021).

In the Figure 2A (40 × magnification), it is possible to see a connective tissue (blueish color) surrounding the biomaterial particles (P) of inorganic bovine bone matrix (IBBM), at the tissue grown inside the tube. Figure 2B represents a 5-fold magnification (200 ×) from a distinctive part at 2A. In the Figure 2B, it is possible to see (redish color) the development of bone deposition, here called immature bone. In Figures 2C (40 ×) and 2D (200 ×), the red color clearly shows a neoformed mature bone deposition around the IBBM particles.

Figure 3 (A-D) demonstrates the results from experimental groups IBBM+MOE3 and IBBM+MOE6. It is possible to note (Figures 3A and 3B) that experimental implants of IBBM+MOE3 promoted the formation of large quantities of collagen fibers along with sparse formation of immature bone, 3 months after implantation. After six months of implantation (Figures 3C and 3D), IBBM+MOE6 were capable to promote the formation of large quantities of osteoid matrix and mature bone at the surface of the remnant particles and in-between them.

Figure 3. Masson trichrome colored histology images from groups 3 and 6 (IBBM + MOE). Images A-B correspond to IBBM + MOE at 3 months. Images C-D correspond to IBBM + MOE at 6 months. In both cases, images are presented in terms of increasing magnification (40 × and 200 ×, respectively). Star = Dense connective tissue; NB = Neoformed mature bone; P = Graft particles; IBM = Inorganic bovine matrix (IBBM); ME = Marine organic extract (MOE).

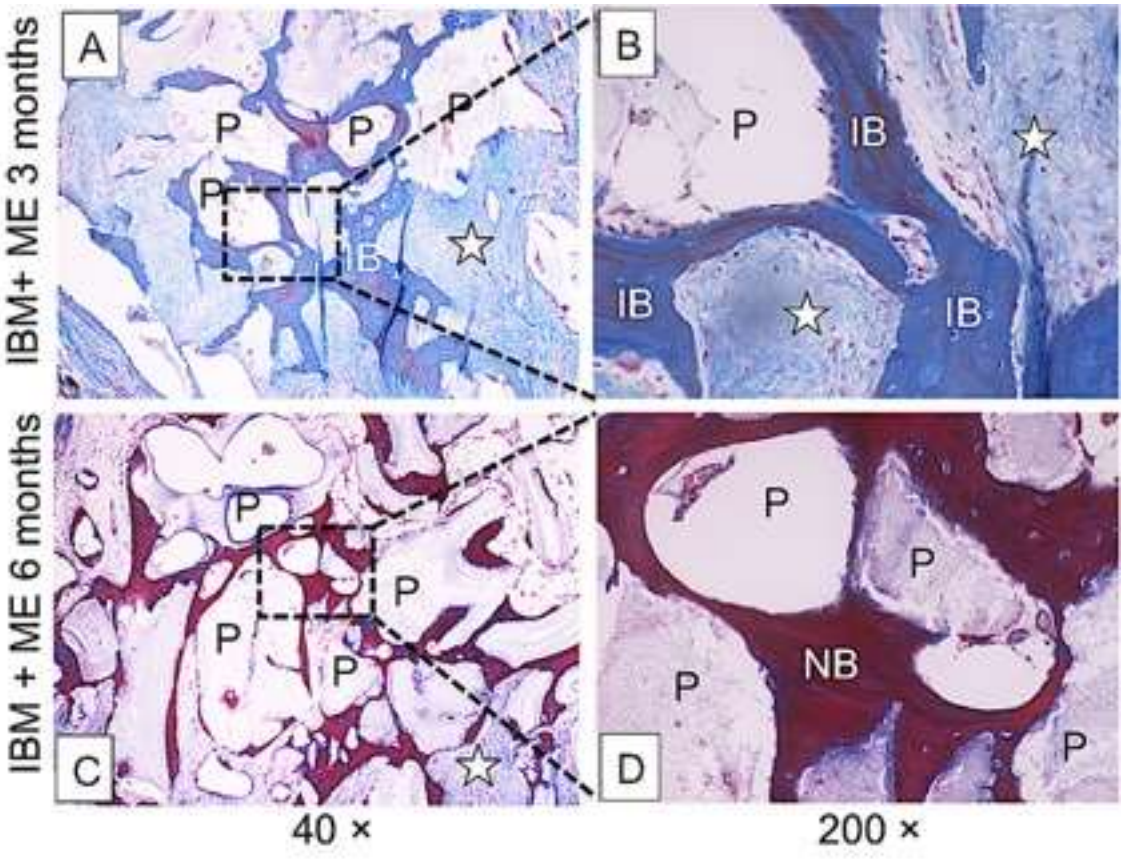

Source: Authors (2021).

In this Figure 3A, it is possible to see that immature bone (dense blueish) is growing around the particles of biomaterial (40 ×, Figure 3A; and 200 ×, Figure 3B) after the 3-month period. Figures 3C and 3D (40 × and 200 ×, respectively) demonstrate a redish and mature bone around de inorganic particles of the biomaterial, after the 6-month period.

3.2 Histomorphometric findings

The histomorphometric analysis performed for all groups investigated was made necessary to allow for the calculation of the (i) total area analyzed (in terms of pixels^2 [px^2]) and the relative quantities of (ii) remnant particles, and (iii) neoformed bone presented inside of the non-reactive polyethylene carriers after implantation (at 3 or 6 months). Results obtained indicate that the total area analyzed for S3, S6, IBBM3, IBBM6 IBBM+MOE3 and IBBM+MOE6 corresponded to 16.27×10^4 px^2, 15.0×10^4 px^2, 46.4×10^4 px^2, 46.7×10^4 px^2, 53.1×10^4 px^2 and 50.2×10^4 px^2, respectively, which demonstrate that amounts of tissues formed inside of implants pertaining to groups with IBBM (unaltered of MOE-modified; at either 3 or 6 months) were higher and statistically significant ($p < 0.05$), when compared to the amount of tissues formed in groups S3 and S6 (negative controls; Figure 4). Statistical

significant differences could not be observed ($p > 0.05$) when types of implants (S3-IBBM+MOE6) was considered for the calculation of the parameter "total area".

Figure 4. Tissue formation inside of the non-reactive polyethylene tubes. Sham = Control group; IBBM = Inorganic bovine matrix; IBBM + MOE = Inorganic bovine matrix with marine organic extract. Mean values with different letters are statistically different ($p < 0.05$).

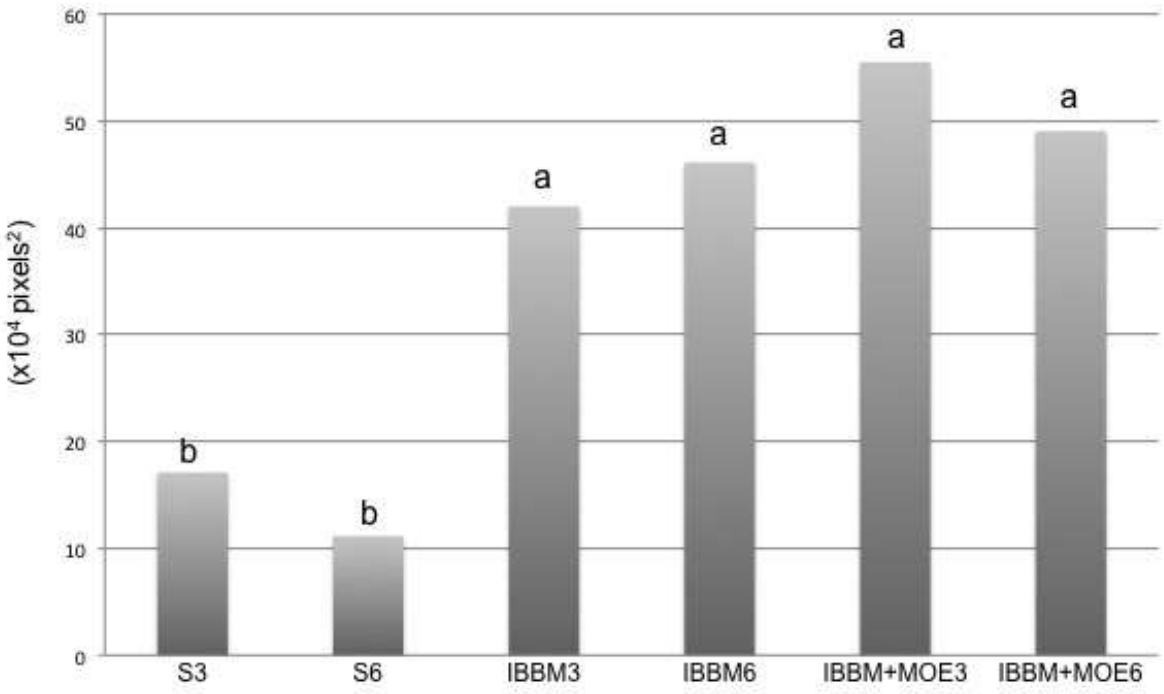

Source: Authors (2021).

Figure 4 shows a comparative of the remnant tissue taken from inside the tubes in each situation, without any biomaterial (Sham) and with biomaterial (IBBM and IBBM+MOE). It clearly shows that the presence of biomaterial (IBBM and IBBM+MOE) makes all the difference in the maintenance of area occupied inside the tubes.

For the parameter "remnant particles", the results show that implants of groups IBBM3, IBBM6, IBBM+MOE3 and IBBM+MOE6 displayed 39.7%, 43.2%, 32.6% and 27.7%, respectively, which indicate that implants containing MOE-modified IBBM displayed the lowest amounts of remnant particles present inside the non-reactive carriers, independently of time considered (either 3 or 6 months). The parameter "neoformed bone" was demonstrated to have a relative area of 0.4% (IBBM3), 7.3% (IBBM6), 11.8% (IBBM+MOE3) and 19.2% (IBBM+MOE6), respectively, which indicates that implants containing experimental materials modified by MOE displayed mineralized bony tissues in quantities that were significantly ($p < 0.05$) higher, when compared to implants of positive controls (IBBM3 and IBBM6), while negative controls did not produce any bone at all (S3 and S6).

3.3 Immunohistochemical findings

The results from the immunohistochemical analysis are reported in Table 2. It is possible to observe that the combination between the parameters "time" (either 3 or 6 months) and "implant type" (Sham, IBBM or IBBM + MOE) did not result in differences

that were statistically significant ($p > 0.05$), independently of the antibody considered (CD34, vimentin, Wnt3a, Pref-1). However, when the factors "time" (either 3 or 6 months) and "implant type" (Sham, IBBM or IBBM + MOE) were individually analyzed, statistically significant differences ($p = 0.024$ and $p = 0.005$, respectively) were observed for the expression of the antibody Wnt3a. The *post hoc* used (Tukey test) was able to further discriminate ($p = 0.02$) differences observed, and indicated that implants of negative controls (Sham) displayed the lowest Wnt3a expression (7.83 ± 0.58) when compared to implants containing either IBBM (9.89 ± 0.43) or MOE-modified IBBM (9.68 ± 0.43). Figure 5 (A-E; Wnt3a) illustrates representative images of slides prepared for immunohistochemical analysis of tissues in S3 (5A), S6 (5B), IBBM6 (5C), IBBM+MOE3 (5D) and IBBM3 (5E).

Table 2. Results from the immunohistochemical analysis (pixels × $10^6)^2$. Data were statistically analyzed using Two-way ANOVA and Tukey post hoc tests with a significance level of 0.05. Numbers in rows followed by similar lower case letters are not statistically different ($p > 0.05$). Numbers displaying similar capital letters within columns are not statistically different ($p > 0.05$).

Groups	Time	Biomaterial (abbreviation)	CD34 (pixels x 10^6)^2	Vimentin (pixels x 10^6)^2	PREF1 (pixels x 10^6)^2	Wnt3a (pixels x 10^6)^2
1	3 mos.	Sham (S3)	8.50 ± 1.03^{aA}	6.49 ± 2.49^{aA}	8.52 ± 4.25^{aA}	8.38 ± 1.50^{aA}
2		IBBM (IBBM3)	5.16 ± 4.53^{aA}	10.31 ± 0.06^{aA}	12.39 ± 1.16^{aA}	9.93 ± 0.60^{aA}
3		IBBM + MOE (IBBM+MOE3)	6.20 ± 0.38^{aA}	9.10 ± 2.10^{aA}	10.55 ± 0.28^{aA}	11.05 ± 1.72^{aA}
4	6 mos.	Sham (S6)	5.66 ± 4.73^{aA}	10.50 ± 1.81^{aA}	0.67 ± 4.51^{aA}	6.92 ± 1.76^{aA}
5		IBBM (IBBM6)	10.19 ± 1.66^{aA}	8.52 ± 2.21^{aA}	14.85 ± 1.16^{aA}	9.71 ± 0.81^{aA}
6		IBBM + MOE (IBBM+MOE6)	9.08 ± 1.87^{aA}	8.32 ± 2.58^{aA}	11.88 ± 2.04^{aA}	6.61 ± 2.63^{aA}

Source: Authors (2021).

Table 2 shows the overall quantitative results of all immunohistochemical analysis while comparing all of the groups. No difference was observed, neither at 3 nor at 6 months for any of the antibodies used.

Figure 5. Representative images from the immunohistochemical analysis for (A) Sham at 3 months, (B) Sham at 6 months, (C) IBBM at 6 months, (D) IBBM + MOE at 3 months and (E) IBBM at 3 months. Images indicate positive staining for Wnt3a.

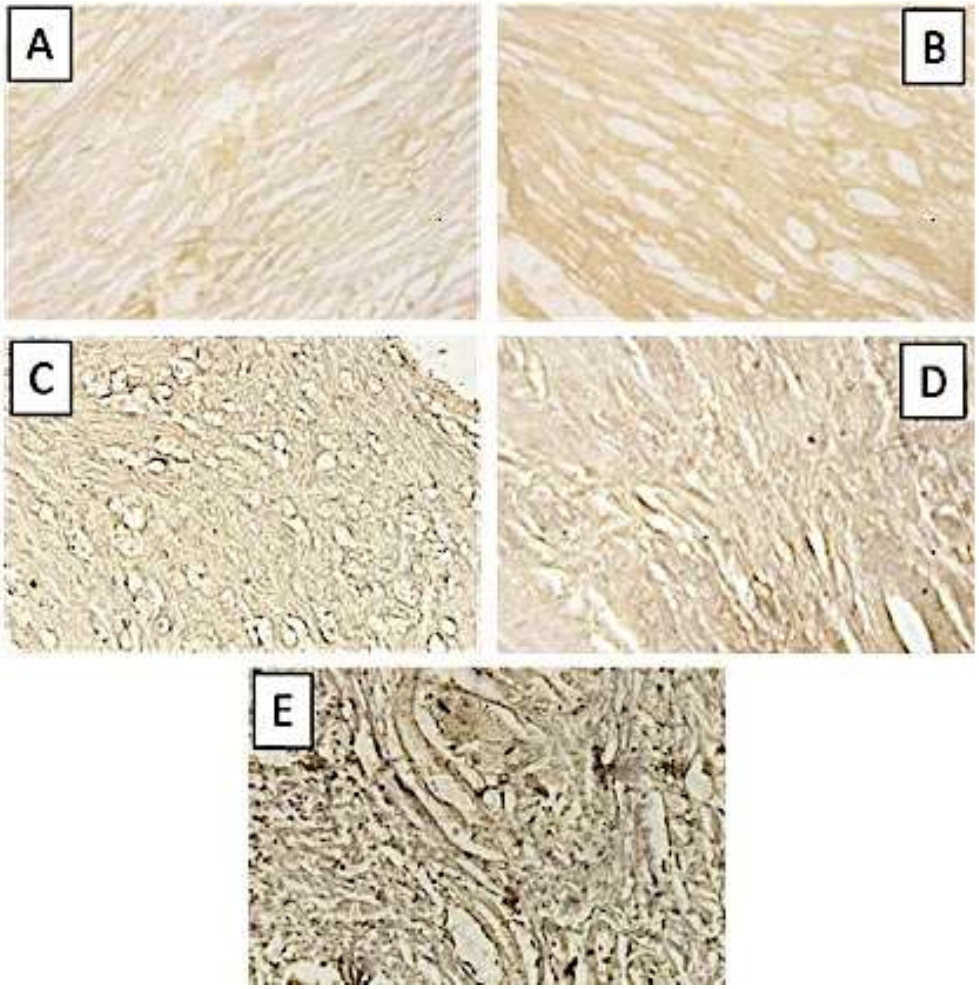

Source: Authors (2021).

Figure 5 shows separate slides of extracellular matrix immunohistochemical positive staining (5A and 5B = Sham 3 and Sham 6 months, respectively), which can demonstrate that in the presence of the biomaterial (5C = IBBM at 6 months, D = IBBM + MOE at 3 months and 5E = IBBM at 3 months) the Wnt3a marker was stronger.

4. Discussion

The ectopic sheep model used allowed to investigate the osteoinductive, osteoconductive and trans-differentiation properties of materials investigated (S3, S6, IBBM3, IBBM6, IBBM+MOE3 and IBBM+MOE6) after 3 or 6 months of intramuscular implantation. The experimental design utilized also allowed the assessment of the presence of inflammatory reactions in adjacent tissues, which were not observed in any of the slides or groups. The rationale for the selection of the experimental design used was based on the fact that such implantation model mimics unstable mechanical environments (Wu et al., 2011), limit the mechanical interference of the host, display abundant blood irrigation, and can be used to assess the biocompatibility and osteoinductive properties of implantable biomaterials (Habibovic et al., 2008; Lioubavina-Hack et al., 2005). Other studies (Le Nihouannen et al.,

2005; Martini et al., 2001) have shown that ectopic sheep models are convenient, fast, efficient and provide testing conditions that are comparable to those of humans. In addition, sheep models display undisputable sensitivity to screen for foreign-body reactions (i.e., giant cells, formation of fibrous connective tissues and macrophage accumulation) (Anderson et al., 2008). No reaction such as foreign-body was observed in the present study for the control (sham) or experimental groups with IBBM particles.

The selection of non-reactive sterile polyethylene tubes as a method to deliver experimental biomaterials investigated was based on previous reports from our laboratory (da Silva et al., 2016; Zielak et al., 2018) demonstrating that tubes of similar compositions, implanted under comparable conditions, did not trigger allergic or inflammatory reactions of any kind. In the present study, inflammatory reactions adjacent to the implants could not be observed, independently of the material considered (S3, S6, IBBM3, IBBM6, IBBM+MOE3 and IBBM+MOE6) or implantation time (either 3 or 6 months). Therefore, these implants are in agreement with previous reports (da Silva et al., 2016; Donaruma, 1988; Zielak et al., 2018), and further validate the utilization of sterile inert polyethylene tubes for the investigation of osteoconductive and osteoinductive properties of implantable biomaterials (either experimental or commercially available). The rationale for the selection of IBBM as the immobilizing agent for the experimental nacre extract was based on previous reports (Marins et al., 2004; Trotta et al., 2014) showing that these types of implantable biomaterials do not induce the formation of inflammatory lymphocyte cells. Again, the results reported in the current study are in agreement with the studies cited (Marins et al., 2004; Trotta et al., 2014), once the presence of inflammatory cells were not observed adjacent to implants, independently of the "time" or "implant type" considered.

Although not quantified, the Figures 2 (IBBM3 and IBBM6) and 3 (IBBM+MOE3 and IBBM+MOE6) illustrate the presence of osteoid matrix. In addition to that, our findings also indicate that implants of IBMM6 induced the formation of sparsely distributed neoformed bone among remnant particles, thereby suggesting that unaltered IBBM (without MOE) display promising osteoinductive properties. These results contradict previously published reports indicating that IBBM only display osteoconductive properties (Baron & Kneissel, 2013; Carvalho et al., 2004). According to its manufacturer (Baumer, Brazil), the IBBM (GenOx Inorg®, Baumer, Brazil) used in the present study display superior biological properties, because of the combination between high sintering temperatures (1,000°C) and the controlled processing conditions (not disclosed), which can result in highly crystalline and porous (100-250 μm) inorganic material, capable of facilitating the adhesion of cells (Zambuzzi et al., 2012), while improving the contact area (Galindo-Moreno et al., 2013) between IBBM particles and MOE.

Rosa et al. (2000) while investigating the effect of powder processing and sintering conditions on the porosity of experimental hydroxyapatite scaffolds, demonstrated that parameters investigated (either temperature and load) were inversely correlated to porosity size. Aarthy et al. (2019) while exploring the effect of sintering temperatures on the properties of naturally derived hydroxyapatite materials, have shown that bioactivity was proportionally correlated to sintering temperature where higher temperatures resulted in materials displaying stronger bioactivity properties. Other studies suggest that high-temperature (> 900°C) treatments may negatively affect the crystalline structure of hydroxyapatite and their biological properties (Figueiredo et al., 2010; Lopez-Heredia et al., 2011), which may be used to partially explain the variability associated with the osteoconductive and osteoinductive properties of commercially available products.

The results of the histological assessment presented in Figures 1-3 suggest that the parameter "remnant particles" inversely varied in function of "time" and "implant type" (IBBM3 < IBBM6 < IBBM+MOE3 < IBBM+MOE6). In addition, the results reported have clearly shown that implants of IBBM3 and IBBM+MOE6 displayed, respectively, the highest and lowest amounts of remnant particles amongst all groups investigated. Such findings suggest that the utilization of MOE (40 μL/implant) may have

upregulated (i) osteoclasts activity, (ii) the expression of degradation pathways and (iii) bone remodeling, thereby overcoming some typical limitations of IBBM (e.g., low resorption rates) (Anderson et al., 2000). Other studies investigating the biomineralization properties of marine biomaterials have indicated that longer implantation times typically result in higher levels of osteoclastic activity, and smaller quantities of mineralized particles, and therefore, have corroborated with the findings of the present study (Asvanund, 2011; de Almeida, 2011; Oliveira et al., 2012; Rousseau, 2011; Zhang et al., 2017; Zielak et al., 2018).

In regards to the parameter "bone neoformation", the results reported (Figure 4) have indicated that implants of IBBM+MOE (at 3 or 6 months) displayed amounts of neoformed bone that were significantly ($p < 0.05$) higher when compared to implants pertaining to control groups (S3, S6, IBBM3 and IBBM6). Implants of IBBM+MOE6 displayed the highest amount of neoformed bone, vascular tissues and mature bone, which suggest that IBBM and MOE might have a synergistic biomineralization effect when implanted for at least six months. The findings reported in the present study have been corroborated by previous studies (Chaturvedi et al., 2013; Wang & Cooke, 2005) investigating the ability of marine organo-biomaterials to stimulate bone formation. According to the studies cited (Chaturvedi et al., 2013; Wang & Cooke, 2005), nacre extracts display favorable biochemical properties (e.g., high bioavailability and low resorption) that are capable to modulate specific biological reactions, thereby resulting in high levels of bone formation.

The findings reported for the immunohistochemical analysis are presented in Table 2 and Figure 5. Even though statistical differences could not be found ($p > 0.05$) for the expression of overall antibodies among the groups investigated, it can be noted that higher mean absolute values for CD34 were associated with implants of IBBM6 and IBBM+MOE6, which may suggest that, even in longer periods, IBBM particles continue to stimulate angiogenesis. Such statement has been corroborated by a previous study (Seifi et al., 2011) investigating the density of microvessels in follicular cysts. According to results reported, higher expressions of CD34 are positively and strongly correlated with the presence of immature vascular tissues (Seifi et al., 2011). Regarding Vimentin antibodies, although S6 displayed the highest mean absolute values, the total tissue area was still much smaller (15.0×10^4 px^2) than the groups with IBBM particles, which is compatible to the morphological characteristic of a thinner but dense and organized connective tissue found inside the non-reactive carriers pertaining to the Sham groups. In addition to that, and based on these findings (no significant differences among all antibodies, including Vimentin, Table 2), it may be inferred that the experimental materials investigated (IBBM or IBBM+MOE) did not present any potential to stimulate fibroblasts transdifferentiation into osteoblasts, either at 3 or 6 months after intramuscular implantation.

Significant statistical differences were only found ($p < 0.05$) when Wnt3a antibodies were analyzed separately. According to Nusse and Varmus (2012), the presence of mature bone naturally downregulates the overall expression of Wnt3a. Thus, although IBBM+MOE6 group displayed the lowest mean absolute value, which can be hypothesized to occur as a direct result of the influence of MOE and its ability to positively modify the biological response of young cells to induce the formation of mature bone (at 6 months), leading to faster osseo-differentiation, data shows that Sham groups (3 and 6 mos.) presented the lowest Wnt3a antibody levels ($p = 0.02$), when compared do IBBM and IBBM+MOE groups - this is in accordance to neoformed bone found only within these groups, supporting the presence of osseo-differentiation (mesenchymal stem cells present within the muscle into osteoblasts).

Also, the absence of osteoid matrix in the group treated with IBBM+MOE can be explained by the typical dissolution behavior of water-soluble materials, their limited bioavailability and restricted long-term biological properties. In this direction, the experimental MOE investigated could be promoting stronger cell based on faster differentiation. IBBM+MOE groups did not result in abnormal or atypical neoformation of bone, and seemed not to display a constant signaling. Thus, regarding these biosafety characteristics, previous reports (Zielak et al., 2018) have indicated that MOE did not induce to mineral deposition or neoformation

of bone when associated with an organic scaffold, which means its efficiency for osseo-induction is probably a calcium/phosphate-dependent. These results regarding Wnt3a are also supported by previous scientific evidence (Jing et al., 2015; Leucht et al., 2013; Miclea et al., 2010; Morvan et al., 2006) that investigated the effects of Wnt3a on the osteogenic capacity of bone graft materials extracted from aged animals.

5. Conclusion

The results of the present study suggest that materials investigated (IBBM and IBBM+MOE) display promising osteoconductive and osteoinductive functionalities that may translate into bone graft materials with superior biological properties. Materials investigated were not observed to display transdifferentiation properties or to trigger the development of inflammatory reactions in adjacent tissues. Despite these promising properties, additional studies are made necessary to characterize the longitudinal effects of materials investigated, their long-term cytotoxic properties and to support the execution of human clinical trials. Other studies from our research group will investigate the effects of biomaterials herein described on mesenchymal stem cells to support the continuous development and characterization of properties.

Acknowledgments

The present study was partially funded by the Curityba Biotech Company and a research grant from the Brazilian Innovation Agency (FINEP # 0986/08).

References

Aarthy, S., Thenmuhil, D., Dharunya, G., & Manohar, P. (2019). Exploring the effect of sintering temperature on naturally derived hydroxyapatite for bio-medical applications [journal article]. *Journal of Materials Science: Materials in Medicine, 30*(2), 21. https://doi.org/10.1007/s10856-019-6219-9

Addadi, L., Joester, D., Nudelman, F., & Weiner, S. (2006). Mollusk Shell Formation: A Source of New Concepts for Understanding Biomineralization Processes. *Chemistry – A European Journal, 12*(4), 980-987. https://doi.org/10.1002/chem.200500980

Akiyama, T., Sato, S., Chikazawa-Nohtomi, N., Soma, A., Kimura, H., Wakabayashi, S., Ko, S. B. H., & Ko, M. S. H. (2018). Efficient differentiation of human pluripotent stem cells into skeletal muscle cells by combining RNA-based MYOD1-expression and POU5F1-silencing. *Scientific reports, 8*(1), 1189-1189. https://doi.org/10.1038/s41598-017-19114-y

Anderson, H. C., Hodges, P. T., Aguilera, X. M., Missana, L., & Moylan, P. E. (2000). Bone morphogenetic protein (BMP) localization in developing human and rat growth plate, metaphysis, epiphysis, and articular cartilage. *J Histochem Cytochem, 48*(11), 1493-1502. https://doi.org/10.1177/002215540004801106

Anderson, J. M., Rodriguez, A., & Chang, D. T. (2008, 2008/04/01/). Foreign body reaction to biomaterials. *Seminars in Immunology, 20*(2), 86-100. https://doi.org/https://doi.org/10.1016/j.smim.2007.11.004

Asvanund, P. C., P. Suddhasthira, T. (2011). Potential induction of bone regeneration by nacre: an in vitro study. *Implant Dent, 20*(1), 32-39. https://doi.org/10.1097/ID.0b013e3182061be1

Atlan, G., Balmain, N., Berland, S., Vidal, B., & Lopez, É. (1997, 1997/03/01/). Reconstruction of human maxillary defects with nacre powder: histological evidence for bone regeneration. *Comptes Rendus de l'Académie des Sciences - Series III - Sciences de la Vie, 320*(3), 253-258. https://doi.org/https://doi.org/10.1016/S0764-4469(97)86933-8

Baron, R., & Kneissel, M. (2013). WNT signaling in bone homeostasis and disease: from human mutations to treatments. *Nat Med, 19*(2), 179-192. https://doi.org/10.1038/nm.3074

Beauchamp, J. R., Heslop, L., Yu, D. S. W., Tajbakhsh, S., Kelly, R. G., Wernig, A., Buckingham, M. E., Partridge, T. A., & Zammit, P. S. (2000). Expression of Cd34 and Myf5 Defines the Majority of Quiescent Adult Skeletal Muscle Satellite Cells. *The Journal of Cell Biology, 151*(6), 1221-1234. https://doi.org/10.1083/jcb.151.6.1221

Bennett, C. N., Longo, K. A., Wright, W. S., Suva, L. J., Lane, T. F., Hankenson, K. D., & MacDougald, O. A. (2005). Regulation of osteoblastogenesis and bone mass by Wnt10b. *Proc Natl Acad Sci U S A, 102*(9), 3324-3329. https://doi.org/10.1073/pnas.0408742102

Carvalho, P. S. P. d. C., Bassi, A. P. F., & Pereira, L. A. V. D. (2004). Revisão e proposta de nomenclatura para os biomateriais. *Revista Implant News, 1*(3), 255-260.

Chaturvedi, R., Singha, P. K., & Dey, S. (2013). Water Soluble Bioactives of Nacre Mediate Antioxidant Activity and Osteoblast Differentiation. *PLOS ONE, 8*(12), e84584. https://doi.org/10.1371/journal.pone.0084584

Cho, Y. D., Yoon, W. J., Kim, W. J., Woo, K. M., Baek, J. H., Lee, G., Ku, Y., van Wijnen, A. J., & Ryoo, H. M. (2014). Epigenetic modifications and canonical wingless/int-1 class (WNT) signaling enable trans-differentiation of nonosteogenic cells into osteoblasts. *J Biol Chem, 289*(29), 20120-20128. https://doi.org/10.1074/jbc.M114.558064

da Silva, R. C., Crivellaro, V. R., Giovanini, A. F., Scariot, R., Gonzaga, C. C., & Zielak, J. C. (2016). Radiographic and histological evaluation of ectopic application of deproteinized bovine bone matrix. *Ann Maxillofac Surg, 6*(1), 9-14. https://doi.org/10.4103/2231-0746.186150

de Almeida, U., Zielak, J. C., Filietaz, M., Giovanini, A. F., Deliberador, T. M., Ulbrich, L. M., & Gonzaga, C. C. (2011). Biomaterial's analysis and use, made of crassostrea giga shells in rats' periodontal defects. *Odontol. Clín.-Cient., 10*(3), 259-263.

Donaruma, L. G. (1988). Definitions in biomaterials, D. F. Williams, Ed., Elsevier, Amsterdam, 1987, 72 pp. *Journal of Polymer Science Part C: Polymer Letters, 26*(9), 414-414. https://doi.org/10.1002/pol.1988.140260910

Duplat, D., Chabadel, A., Gallet, M., Berland, S., Bedouet, L., Rousseau, M., Kamel, S., Milet, C., Jurdic, P., Brazier, M., & Lopez, E. (2007). The in vitro osteoclastic degradation of nacre. *Biomaterials, 28*(12), 2155-2162. https://doi.org/10.1016/j.biomaterials.2007.01.015

Fhied, C., Kanangat, S., & Borgia, J. A. (2014). Development of a bead-based immunoassay to routinely measure vimentin autoantibodies in the clinical setting. *J Immunol Methods, 407*, 9-14. https://doi.org/10.1016/j.jim.2014.03.011

Figueiredo, M., Fernando, A., Martins, G., Freitas, J., Judas, F., & Figueiredo, H. (2010, 2010/12/01/). Effect of the calcination temperature on the composition and microstructure of hydroxyapatite derived from human and animal bone. *Ceramics International, 36*(8), 2383-2393. https://doi.org/https://doi.org/10.1016/j.ceramint.2010.07.016

Galindo-Moreno, P., Hernandez-Cortes, P., Mesa, F., Carranza, N., Juodzbalys, G., Aguilar, M., & O'Valle, F. (2013). Slow resorption of anorganic bovine bone by osteoclasts in maxillary sinus augmentation. *Clin Implant Dent Relat Res, 15*(6), 858-866. https://doi.org/10.1111/j.1708-8208.2012.00445.x

Habibovic, P., Kruyt, M. C., Juhl, M. V., Clyens, S., Martinetti, R., Dolcini, L., Theilgaard, N., & van Blitterswijk, C. A. (2008). Comparative in vivo study of six hydroxyapatite-based bone graft substitutes. *J Orthop Res, 26*(10), 1363-1370. https://doi.org/10.1002/jor.20648

Huang, Z., & Li, X. (2012). Order-disorder transition of aragonite nanoparticles in nacre. *Phys Rev Lett, 109*(2), 025501. https://doi.org/10.1103/PhysRevLett.109.025501

Jasani, B. (2000). Manual of Diagnostic Antibodies for Immunohistology: Leong AS-Y, Cooper K, Joel F, Leong W-M. (£45.00.) Oxford University Press, 1999. ISBN 1 900151 31 6. *Molecular Pathology, 53*(1), 53-53. https://www.ncbi.nlm.nih.gov/pmc/articles/PMC1186905/

Jing, W., Smith, A. A., Liu, B., Li, J., Hunter, D. J., Dhamdhere, G., Salmon, B., Jiang, J., Cheng, D., Johnson, C. A., Chen, S., Lee, K., Singh, G., & Helms, J. A. (2015). Reengineering autologous bone grafts with the stem cell activator WNT3A. *Biomaterials, 47*, 29-40. https://doi.org/10.1016/j.biomaterials.2014.12.014

Lagace, R., Grimaud, J. A., Schurch, W., & Seemayer, T. A. (1985). Myofibroblastic stromal reaction in carcinoma of the breast: variations of collagenous matrix and structural glycoproteins. *Virchows Arch A Pathol Anat Histopathol, 408*(1), 49-59.

Le Nihouannen, D., Daculsi, G., Saffarzadeh, A., Gauthier, O., Delplace, S., Pilet, P., & Layrolle, P. (2005, 2005/06/01/). Ectopic bone formation by microporous calcium phosphate ceramic particles in sheep muscles. *Bone, 36*(6), 1086-1093. https://doi.org/https://doi.org/10.1016/j.bone.2005.02.017

Lee, J., Choi, W. I., Tae, G., Kim, Y. H., Kang, S. S., Kim, S. E., Kim, S. H., Jung, Y., & Kim, S. H. (2011). Enhanced regeneration of the ligament-bone interface using a poly(L-lactide-co-epsilon-caprolactone) scaffold with local delivery of cells/BMP-2 using a heparin-based hydrogel. *Acta Biomater, 7*(1), 244-257. https://doi.org/10.1016/j.actbio.2010.08.017

Leucht, P., Jiang, J., Cheng, D., Liu, B., Dhamdhere, G., Fang, M. Y., Monica, S. D., Urena, J. J., Cole, W., Smith, L. R., Castillo, A. B., Longaker, M. T., & Helms, J. A. (2013). Wnt3a reestablishes osteogenic capacity to bone grafts from aged animals. *J Bone Joint Surg Am, 95*(14), 1278-1288. https://doi.org/10.2106/jbjs.L.01502

Lioubavina-Hack, N., Karring, T., Lynch, S. E., & Lindhe, J. (2005). Methyl cellulose gel obstructed bone formation by GBR: an experimental study in rats. *J Clin Periodontol, 32*(12), 1247-1253. https://doi.org/10.1111/j.1600-051X.2005.00791.x

Lopez, E., Giraud, M., Berland, S., Milet, C., Gutierrez, G. (1996). *Method for preparation of active substances from nacre, resulting products, useful in medicinal applications* (France Patent No. A. f. b. C. N. D. L. R. S. (Cnrs).

Lopez, E., Vidal, B., Berland, S., Camprasse, S., Camprasse, G., & Silve, C. (1992). Demonstration of the capacity of nacre to induce bone formation by human osteoblasts maintained in vitro. *Tissue Cell, 24*(5), 667-679.

Lopez-Heredia, M. A., Kamphuis, G. J., Thune, P. C., Oner, F. C., Jansen, J. A., & Walboomers, X. F. (2011). An injectable calcium phosphate cement for the local delivery of paclitaxel to bone. *Biomaterials, 32*(23), 5411-5416. https://doi.org/10.1016/j.biomaterials.2011.04.010

Marins, L. V., Cestari, T. M., Sottovia, A. D., Granjeiro, J. M., & Taga, R. (2004). Radiographic and histological study of perennial bone defect repair in rat calvaria after treatment with blocks of porous bovine organic graft material. *J Appl Oral Sci, 12*(1), 62-69. https://doi.org/10.1590/s1678-77572004000100012

Martín-Moldes, Z., Ebrahimi, D., Plowright, R., Dinjaski, N., Perry, C. C., Buehler, M. J., & Kaplan, D. L. (2018). Intracellular Pathways Involved in Bone Regeneration Triggered by Recombinant Silk–Silica Chimeras. *Advanced Functional Materials, 28*(27), 1702570. https://doi.org/10.1002/adfm.201702570

Martini, L., Fini, M., Giavaresi, G., & Giardino, R. (2001). Sheep model in orthopedic research: a literature review. *Comp Med, 51*(4), 292-299.

Miclea, R. L., Karperien, M., Langers, A. M., Robanus-Maandag, E. C., van Lierop, A., van der Hiel, B., Stokkel, M. P., Ballieux, B. E., Oostdijk, W., Wit, J. M., Vasen, H. F., & Hamdy, N. A. (2010). APC mutations are associated with increased bone mineral density in patients with familial adenomatous polyposis. *J Bone Miner Res, 25*(12), 2624-2632. https://doi.org/10.1002/jbmr.153

Minear, S., Leucht, P., Jiang, J., Liu, B., Zeng, A., Fuerer, C., Nusse, R., & Helms, J. A. (2010). Wnt proteins promote bone regeneration. *Sci Transl Med, 2*(29), 29ra30. https://doi.org/10.1126/scitranslmed.3000231

Morvan, F., Boulukos, K., Clement-Lacroix, P., Roman Roman, S., Suc-Royer, I., Vayssiere, B., Ammann, P., Martin, P., Pinho, S., Pognonec, P., Mollat, P., Niehrs, C., Baron, R., & Rawadi, G. (2006). Deletion of a single allele of the Dkk1 gene leads to an increase in bone formation and bone mass. *J Bone Miner Res, 21*(6), 934-945. https://doi.org/10.1359/jbmr.060311

Nogami, K., Blanc, M., Takemura, F., Takeda, S., Miyagoe-Suzuki, Y. (2018). Making Skeletal Muscle from Human Pluripotent Stem Cells, Muscle Cell and Tissue. In K. Sakuma (Ed.), *Current Status of Research Field*. IntechOpen. https://doi.org/10.5772/intechopen.77263

Nusse, R., & Varmus, H. (2012, Jun 13). Three decades of Wnts: a personal perspective on how a scientific field developed. *Embo j, 31*(12), 2670-2684. https://doi.org/10.1038/emboj.2012.146

Oliveira, D. V., Silva, T. S., Cordeiro, O. D., Cavaco, S. I., & Simes, D. C. (2012). Identification of proteins with potential osteogenic activity present in the water-soluble matrix proteins from Crassostrea gigas nacre using a proteomic approach. *TheScientificWorldJournal, 2012*, 765909-765909. https://doi.org/10.1100/2012/765909

Reimann, J., Brimah, K., Schroder, R., Wernig, A., Beauchamp, J. R., & Partridge, T. A. (2004). Pax7 distribution in human skeletal muscle biopsies and myogenic tissue cultures. *Cell Tissue Res, 315*(2), 233-242. https://doi.org/10.1007/s00441-003-0833-y

Rosa, A. L., Shareef, M. Y., & van Noort, R. (2000). Efeito das condições de preparação e sinterização sobre a porosidade da hidroxiapatita. *Pesquisa Odontológica Brasileira, 14*, 273-277. http://www.scielo.br/scielo.php?script=sci_arttext&pid=S1517-74912000000300015&nrm=iso

Rousseau, M. (2011). *Nacre, a Natural Biomaterial*. IntechOpen. https://doi.org/10.5772/22978.

Seifi, S., Shafaie, S., & Ghadiri, S. (2011). Microvessel density in follicular cysts, keratocystic odontogenic tumours and ameloblastomas. *Asian Pac J Cancer Prev, 12*(2), 351-356.

Silve, C., Lopez, E., Vidal, B., Smith, D. C., Camprasse, S., Camprasse, G., & Couly, G. (1992). Nacre initiates biomineralization by human osteoblasts maintained in vitro. *Calcif Tissue Int, 51*(5), 363-369. https://doi.org/10.1007/bf00316881

Trotta, D. R., Gorny, C., Jr., Zielak, J. C., Gonzaga, C. C., Giovanini, A. F., & Deliberador, T. M. (2014). Bone repair of critical size defects treated with mussel powder associated or not with bovine bone graft: histologic and histomorphometric study in rat calvaria. *J Craniomaxillofac Surg, 42*(6), 738-743. https://doi.org/10.1016/j.jcms.2013.11.004

Urist, M. R. (1965). Bone: formation by autoinduction. *Science, 150*(3698), 893-899. https://doi.org/10.1126/science.150.3698.893

Urist, M. R., & Strates, B. S. (1970). 29 Bone Formation in Implants of Partially and Wholly Demineralized Bone Matrix: Including Observations on Acetone-fixed Intra and Extracellular Proteins. *Clinical Orthopaedics and Related Research®, 71*, 271-278. https://journals.lww.com/clinorthop/Fulltext/1970/07000/29_Bone_Formation_in_Implants_of_Partially_and.31.aspx

Wang, H. L., & Cooke, J. (2005). Periodontal regeneration techniques for treatment of periodontal diseases. *Dent Clin North Am, 49*(3), 637-659, vii. https://doi.org/10.1016/j.cden.2005.03.004

Wu, G., Hunziker, E. B., Zheng, Y., Wismeijer, D., & Liu, Y. (2011, 2011/12/01/). Functionalization of deproteinized bovine bone with a coating-incorporated depot of BMP-2 renders the material efficiently osteoinductive and suppresses foreign-body reactivity. *Bone, 49*(6), 1323-1330. https://doi.org/https://doi.org/10.1016/j.bone.2011.09.046

Zambuzzi, W. F., Fernandes, G. V., Iano, F. G., Fernandes Mda, S., Granjeiro, J. M., & Oliveira, R. C. (2012). Exploring anorganic bovine bone granules as osteoblast carriers for bone bioengineering: a study in rat critical-size calvarial defects. *Braz Dent J, 23*(4), 315-321.

Zhang, G., Brion, A., Willemin, A. S., Piet, M. H., Moby, V., Bianchi, A., Mainard, D., Galois, L., Gillet, P., & Rousseau, M. (2017). Nacre, a natural, multi-use, and timely biomaterial for bone graft substitution. *J Biomed Mater Res A, 105*(2), 662-671. https://doi.org/10.1002/jbm.a.35939

Zielak, J. C., Neto, D. G., Cazella Zielak, M. A., Savaris, L. B., Esteban Florez, F. L., & Deliberador, T. M. (2018). In vivo regeneration functionalities of experimental organo-biomaterials containing water-soluble nacre extract. *Heliyon, 4*(9), e00776-e00776. https://doi.org/10.1016/j.heliyon.2018.e00776